NEURAL REGENERATION RESEARCH
www.nrronline.org

Research Article

Alexa Fluor 488-conjugated cholera toxin subunit B optimally labels neurons 3–7 days after injection into the rat gastrocnemius muscle

https://doi.org/10.4103/1673-5374.337055
Date of submission: July 25, 2021
Date of decision: November 9, 2021
Date of acceptance: December 15, 2021
Date of web publication: February 28, 2022

Jing-Jing Cui, Jia Wang, Dong-Sheng Xu, Shuang Wu, Ya-Ting Guo, Yu-Xin Su, Yi-Han Liu, Yu-Qing Wang, Xiang-Hong Jing, Wan-Zhu Bai*

From the Contents

Graphical Abstract *Labeling efficiency of Alexa Fluor conjugates of the cholera toxin subunit B*

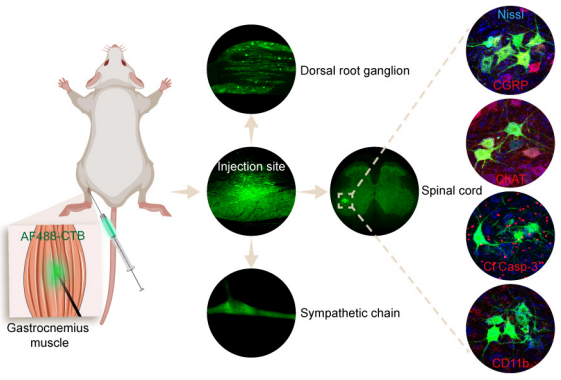

Abstract

Neural tract tracing is used to study neural pathways and evaluate neuronal regeneration following nerve injuries. However, it is not always clear which tracer should be used to yield optimal results. In this study, we examined the use of Alexa Fluor 488-conjugated cholera toxin subunit B (AF488-CTB). This was injected into the gastrocnemius muscle of rats, and it was found that motor, sensory, and sympathetic neurons were labeled in the spinal ventral horn, dorsal root ganglia, and sympathetic chain, respectively. Similar results were obtained when we injected AF594-CTB into the tibialis anterior muscle. The morphology and number of neurons were evaluated at different time points following the AF488-CTB injection. It was found that labeled motor and sensory neurons could be observed 12 hours post-injection. The intensity was found to increase over time, and the morphology appeared clear and complete 3–7 days post-injection, with clearly distinguishable motor neuron axons and dendrites. However, 14 days after the injection, the quality of the images decreased and the neurons appeared blurred and incomplete. Nissl and immunohistochemical staining showed that the AF488-CTB-labeled neurons retained normal neurochemical and morphological features, and the surrounding microglia were also found to be unaltered. Overall, these results imply that the cholera toxin subunit B, whether unconjugated or conjugated with Alexa Fluor, is effective for retrograde tracing in muscular tissues and that it would also be suitable for evaluating the regeneration or degeneration of injured nerves.

Key Words: Alexa Fluor-conjugated cholera toxin subunit B; calcitonin gene-related peptide; microglia; motor neurons; neural tract tracing; optimal time window; sensory neurons; somatotopic organization; sympathetic neurons; tibialis anterior muscle

Introduction

Neural tract tracing is widely used for studying both normal neuronal connections and those that occur following injury, which may reflect neural regeneration or degeneration (Katada et al., 2006; Lanciego and Wouterlood, 2011; Han et al., 2012; Lin et al., 2017; Lanciego and Wouterlood, 2020). There is currently an abundance of commercially-available neural tracers, which have different intrinsic properties. However, it is often unclear which ones should be used to optimally reveal neuronal morphology and pathways (Vercelli et al., 2000; Lanciego and Wouterlood, 2011, 2020).

Alexa Fluor (AF) conjugates of the cholera toxin B subunit (CTB) were developed as neural tracers following the successful use of unconjugated CTB. Their brightness and photostability led them to be extensively used for retrograde tracing within the central nervous system, as well as from the peripheral nervous system to the central nervous system (Dong et al., 2017; Han et al., 2019; Juavinett et al., 2020; Ma et al., 2020; Xu et al., 2021; Zhang et al., 2021). The present study was designed to investigate the use of AF-CTB for studying the peripheral nervous system. The tracers AF488-CTB and AF594-CTB were selected and examined both in isolation and in combination following injection into the gastrocnemius muscle and tibialis anterior muscle in rats. Because the labeling efficiency of tracers varies according to the time interval following the injection (Hirakawa et al., 1992; Zhang et al., 2017), the labeling was evaluated for a series of time points following the injection of AF488-CTB into the gastrocnemius muscle. This would identify an optimal time window for visualizing the labeled neurons in morphological detail.

There is often concern that certain neural tracers may cause pathological changes within the labeled neurons (Puigdellívol-Sánchez et al., 2002; Ling et al., 2012; Hu et al., 2013; Yu et al., 2015; Mi et al., 2019). To examine this, we assessed certain neurochemical substances and the microglia around the AF488-CTB-labeled neurons. This was carried out using fluorescence histochemistry and immunohistochemistry, and we focused on the calcitonin gene-related peptide (CGRP), choline acetyltransferase (ChAT), Nissl, cleaved caspase-3 (Cl Casp-3), and CD11b. The CGRP and ChAT were selected as the neurochemical substances of interest (Zheng et al., 2008; Chen et al., 2010; Li et al., 2019; Das et al., 2021), Nissl and Cl Casp-3 were used to evaluate whether there was degeneration in the labeled neurons (Aras et al., 2012;

Institute of Acupuncture and Moxibustion, China Academy of Chinese Medical Sciences, Beijing, China
*Correspondence to: Wan-Zhu Bai, PhD, wanzhubaisy@hotmail.com.
https://orcid.org/000-0001-6285-7788 (Wan-Zhu Bai)

Funding: *This study was supported by the CACMS Innovation Fund, No. CI2021A03407 (to WZB); the Project of National Key R&D Program of China, No. 2019YFC1709103 (to WZB); the National Natural Science Foundation of China, Nos. 81774432 (to JJC), 81774211 (to WZB), 82004492 (to JW), 81801561 (to DSX); and the Fundamental Research Funds for the Central Public Welfare Research Institutes of China, Nos. ZZ13-YQ-068 (to JJC), ZZ14-YQ-032 (to JW), ZZ14-YQ-034 (to DSX).*
How to cite this article: *Cui JJ, Wang J, Xu DS, Wu S, Guo YT, Su YX, Liu YH, Wang YQ, Jing XH, Bai WZ (2022) Alexa Fluor 488-conjugated cholera toxin subunit B optimally labels neurons 3–7 days after injection into the rat gastrocnemius muscle. Neural Regen Res 17(10):2316-2320.*

Stevenson et al., 2018), and CD11b was used as a pan-microglial marker to assess any morphological alterations in the microglia around the labeled neurons (Köbbert and Thanos, 2000; Sargsyan et al., 2005; Beggs and Salter, 2007; Li et al., 2019). These biomarkers were used to provide histochemical evidence for any pathological changes caused by the tracer.

By determining the optimal conditions for using AF-CTB as a neural tract tracer in the peripheral pathways, it may be possible to improve studies examining neuroanatomical connections and the detailed morphological characteristics of neurons. In addition, by examining whether labeled neurons show any morphological alterations or changes in certain neurochemical substances, this may help to advance our understanding of their functional roles.

Materials and Methods

Ethics statement

This study was approved by the Ethics Committee of the Institute of Acupuncture and Moxibustion, China Academy of Chinese Medical Sciences (approval No. 2021-04-15-1) on April 15, 2021, and carried out in accordance with the National Institutes of Health Guide for the Care and Use of Laboratory Animals (National Academy Press, Washington DC, USA). All of the experiments were designed and reported according to the Animal Research: Reporting of *In Vivo* Experiments (ARRIVE) guidelines (Percie du Sert et al., 2020).

Animals

This study focused on male rats because the cyclic hormonal changes in 2-month-old female rats may affect their physiological state (Sarkar and Mitsugi, 1990). Twenty-seven adult male specific-pathogen-free Sprague-Dawley rats (weight 220–250 g, aged 7–8 weeks) were obtained from the National Institutes for Food and Drug Control (license No. SCXK (Jing) 2017-0005). The rats were provided with free access to food and water, and kept in a 12-hour light-dark cycle with controlled temperature and humidity.

Surgical procedure for tracer injection

The rats were anesthetized by inhalation of 2% isoflurane (YiPin, Shijiazhuang, China) at 0.5 L/min. The body temperature was maintained at 37°C by using a heating pad (Zhike, Zhengzhou, China) during surgery. Twenty-four randomly-selected rats were used for the single-tracer experiment with AF488-CTB. After a small skin incision, 4 μL 0.1% AF488-CTB (Cat# C22841, Invitrogen-Molecular Probes, Eugene, OR, USA) was slowly injected (within 1 minute) into the medial gastrocnemius muscle of the left hind limb. After injection, the needle remained in place for 1 minute to prevent leakage and was then removed. The remaining three rats were used for the dual-tracer experiment, in which 4 μL 0.1% AF488-CTB and AF594-CTB (Cat# C22842, Invitrogen-Molecular Probes) were separately injected into the medial gastrocnemius muscle and the tibialis anterior muscle, respectively, of the same hind limb.

Tissue processing

For the single-tracer experiment, randomly-selected rats were euthanized after 0.5 (12 hours), 1, 2, 3, 5, 7, and 14 days following the AF488-CTB injection (n = 6 after 3 days; n = 3 for the other time points). For dual-tracer experiment using AF488/594-CTB, the three rats were euthanized after 3 days. The rats were anesthetized intraperitoneally with 2,2,2-tribromoethanol (250 mg/kg, Sigma-Aldrich, Darmstadt, Germany) and transcardially perfused with saline followed by a fixative containing 4% paraformaldehyde in 0.1 M phosphate buffer (PB; pH 7.4). The medial gastrocnemius muscle, spinal cord, dorsal root ganglion (DRG), and lumbar sympathetic (paravertebral) chain were dissected and post-fixed for 2 hours using the same fixative, and then cryoprotected overnight in 25% sucrose.

Using a microtome (REM-710, Yamato Koki Industrial, Asaka, Japan), the gastrocnemius muscle was sliced into 80-μm-thick horizontal sections, and the spinal cord was sliced into 40-μm-thick coronal sections. However, for three of the single-tracer rats euthanized on day 3, the spinal cords were sliced into 100-μm-thick horizontal sections. All of the sections were collected in order in a six-hole Petri dish with 0.1 M PB (pH 7.4). As the DRG and the sympathetic chain are both small and transparent, the AF488-CTB- and AF594-CTB-labeled neurons were directly observed in whole-mounts using a fluorescence microscope or confocal imaging system. The DRG from days 3 and 14 were then sliced into 40-μm-thick longitudinal sections for further examination, but the sympathetic chains were not sliced.

Free-floating sections from every sixth spinal coronal section and all of the spinal horizontal sections were mounted on silane-coated glass slides; these were then coverslipped with 50% glycerin to better visualize the labeled neurons.

Fluorescence histochemical and immunohistochemical staining

Fluorescence histochemical or immunohistochemical staining was carried out on the sections of gastrocnemius muscle, spinal cord, and DRG.

The gastrocnemius muscle sections were stained with α-bungarotoxin AF 647 (1:500; Cat# B35450; Life Technologies Corporation, Waltham, MA, USA) and 4′,6-diamidino-2-phenylindole (1:50,000; Cat# D3570; Thermo Fisher, Waltham, MA, USA) for 2 hours at room temperature. The spinal cord and DRG sections from days 3 and 14 were examined for Nissl, CGRP, ChAT, Cl Casp-3, and CD11b, and carried out as follows: (1) CGRP + Nissl to label the motor and sensory neurons; (2) ChAT + Nissl to label the motor neurons; (3) Cl Casp-3 + Nissl to show neuronal degeneration; and (4) CD11b + Nissl to show the microglia around the labeled neurons.

For (1), the DRG sections and spinal sections were both stained; for the others, the spinal sections were stained without the DRG. The staining involved incubating the sections in a blocking solution containing 3% normal donkey serum and 0.5% Triton X-100 in 0.1 M PB (pH 7.4) for 1 hour. The sections were then separately transferred to mouse anti-CGRP monoclonal antibody (1:1000; Cat# ab81887; RRID: AB_1658411; Abcam, Hong Kong Administrative Region, China), goat anti-ChAT (1:100; Cat# AB144P; RRID: AB_2079751; Millipore, Temecula, CA, USA), rabbit anti-Cl Casp-3 (1:500; Cat# 9661S; RRID: AB_2341188; Cell Signaling Technology, Danvers, MA, USA), or mouse anti-CD11b (1:1000; Cat# MCA275R; RRID: AB_321302; Bio-Rad, Hercules, CA, USA) in a dilution of 0.1 M PB containing 1% normal donkey serum and 0.5% Triton X-100, and left overnight at 4°C. The following day, after washing three times with 0.1 M PB, the sections were exposed to the secondary antibodies of donkey anti-mouse AF 594 (1:500; Cat# A21203; RRID: AB_141633; Thermo Fisher), donkey anti-goat AF 594 (1:500; Cat# A11058; RRID: AB_2534105; Thermo Fisher), donkey anti-rabbit AF 594 (1:500; Cat# A21207; RRID: AB_141637; Thermo Fisher), and Nissl AF435/455 (1:1000; Cat# N21479; Thermo Fisher) for 2 hours at room temperature, then washed with 0.1 M PB. The sections were then mounted on the microscope slides and coverslipped with 50% glycerin.

Sample observation

The samples were viewed using the Virtual Slide System (VS120, Olympus, Tokyo, Japan), and representative regions were selected to view in more detail using a confocal imaging system (FV1200, Olympus). The images were collected in successive frames of 5 μm for the whole-mount DRG, sympathetic chain, and longitudinal spinal sections, and in frames of 2 μm for the coronal spinal sections and the longitudinal DRG sections; these were then integrated into a single in-focus image. All of the images were analyzed using the Olympus Image Processing Software and processed using Adobe Photoshop/Illustration CS5 (Adobe Systems, San Jose, CA, USA). The quality of the neuronal labeling was mainly judged according to the morphology of the labeled motor neurons, especially their dendritic branches.

Data analysis

No statistical methods were used to predetermine the sample sizes; however, our sample sizes are similar to those reported in a previous publication (Hirakawa et al., 1992). The data analyses were carried out by a researcher who was blinded as to the experimental group of each image. The statistical analyses were performed using GraphPad Prism 8 software (GraphPad Prism Software, La Jolla, CA, USA). The data were expressed as the mean ± standard error of the mean (SEM). The number of labeled motor and sensory neurons were determined for the 21 rats injected with AF488-CTB. For this, the motor neurons were counted in every sixth slice from the spinal cord, and the sensory neurons were counted in the whole-mount DRG.

Results

Distribution of AF488-CTB around the injection site

The distribution of AF488-CTB labeling around the injection site was examined in the gastrocnemius muscle; this showed the distribution to be limited to an area 6–7 mm in diameter (**Figure 1A**). Histochemical staining with fluorescent α-bungarotoxin revealed the neuromuscular junctions, which were observed using laser scanning confocal microscopy. It was found that the AF488-CTB and α-bungarotoxin labeled the axon terminals and motor endplates, respectively; these were seen to form a branched-pattern together (**Figure 1B** and **B1**).

Distribution of labeled neurons

In the single-tracer experiment, with the injection of AF488-CTB into the gastrocnemius muscle, the labeled neurons were found to include motor, sensory, and sympathetic neurons (**Figure 2**). All of the labeled neurons were located ipsilateral to the injection, and they were distributed in a segmental or regional pattern. They included motor neurons located in the spinal ventral horn in lumbar (L) segments L3–L5, sensory neurons in the L3–L6 DRG, and sympathetic neurons in the lumbar sympathetic chain.

In the dual-tracer experiment, with injections of AF488-CTB and AF594-CTB into the gastrocnemius muscle and the tibialis anterior muscle, respectively, the labeled neuronal components were found to be similar. However, the motor, sensory, and sympathetic neurons that were labeled from the different muscles were distributed separately in their corresponding spinal ventral horn, DRG, and sympathetic chain (**Figure 3**). The motor neurons associated with the tibialis anterior muscle were found to be located more exteriorly within in the spinal ventral horn than those associated with the gastrocnemius muscle; the sensory neurons associated with the tibialis anterior muscle and the gastrocnemius muscle were concentrated in the L4 and L5 DRG, respectively; the sympathetic neurons associated with each muscle were scattered separately throughout the lumbar sympathetic chain (**Figure 3**).

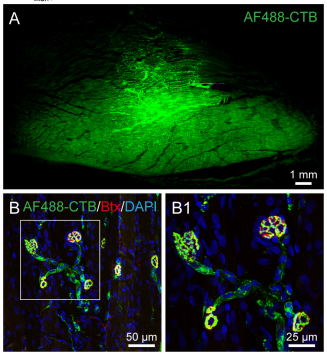

Figure 1 | Distribution of AF488-CTB labeling around the injection site, and labeled neuromuscular junctions in the gastrocnemius muscle on the third day post-injection.
(A) Representative section from the gastrocnemius muscle showing the distribution of AF488-CTB around the injection site. (B) The axon terminals are labeled with AF488-CTB (green) and the motor endplates are labeled with α-bungarotoxin (Btx, red); the background shows DAPI-staining (blue). (B1) Higher magnification of the boxed region in panel B showing the labeled neuromuscular junctions in detail. The images were obtained from an experiment that used three rats. Scale bars: 1 mm in A; 50 μm in B; 25 μm in B1. AF: Alexa Fluor; CTB: cholera toxin subunit B; DAPI: 4′,6-diamidino-2-phenylindole.

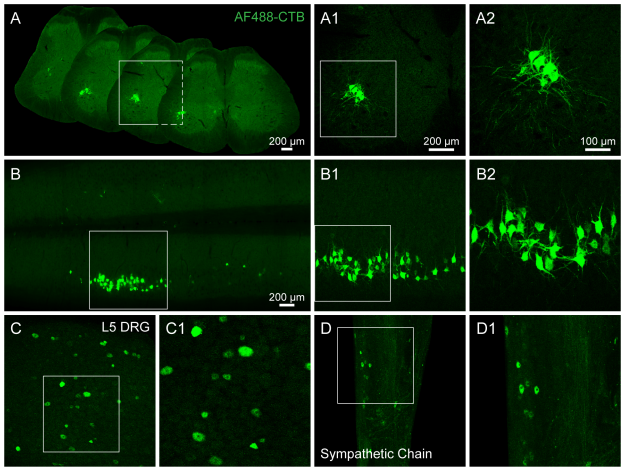

Figure 2 | Distribution of AF488-CTB-labeled motor, sensory, and sympathetic neurons on the third day after the AF488-CTB injection into the gastrocnemius muscle.
(A–D) Representative sections: (A) a series of coronal sections from the spinal cord, (B) a horizontal section from the spinal cord, (C) a whole-mount dorsal root ganglion (DRG) from lumbar (L) segment L5, and (D) a lumbar sympathetic chain. (A1–D1) Higher magnification of the boxed regions in panels A–D showing the labeled neurons in more detail. (A2, B2) Higher magnification of the boxed regions in panels A1 and B1. The images were obtained from an experiment that used three rats. Scale bars: 200 μm in A1, B1, C, and D; 100 μm in A2, B2, C1, and D1. AF: Alexa Fluor; CTB: cholera toxin subunit B.

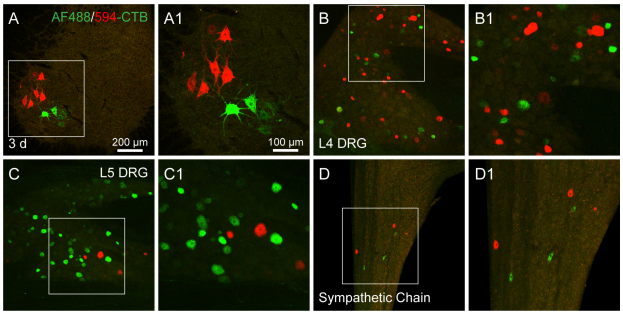

Figure 3 | Distribution of labeled motor, sensory, and sympathetic neurons on the third day after the injection of AF488-CTB and AF594-CTB into the gastrocnemius muscle and tibialis anterior muscle, respectively.
(A–D) Representative sections: (A) a coronal section from the spinal cord, (B) a whole-mount dorsal root ganglion (DRG) from lumbar (L) segment L4, (C) a whole-mount DRG from L5, and (D) a lumbar sympathetic chain. These sections show the distribution of motor (A), sensory (B, C), and sympathetic (D) neurons that were labeled by tracer injections into the gastrocnemius muscle (AF488-CTB) and the tibialis anterior muscle (AF594-CTB). The motor neurons associated with the tibialis anterior muscle are located more exteriorly in the spinal ventral horn than those associated with the gastrocnemius muscle (A); the sensory neurons associated with the tibialis anterior muscle are concentrated in the L4 DRG (B), while those associated with the gastrocnemius muscle are concentrated in the L5 DRG (C); the sympathetic neurons associated with each muscle were scattered separately throughout the lumbar sympathetic chain (D). (A1–D1) Higher magnification of the boxed regions in panels A–D showing the labeled neurons in more detail. The images were obtained from an experiment that used three rats. Scale bars: 200 μm in A–D; 100 μm in A1–D1. AF: Alexa Fluor; CTB: cholera toxin subunit B.

Neuronal morphology

Neuronal labeling with AF488-CTB was evaluated for the motor and sensory neurons at different time points following the AF488-CTB injection (**Figures 4** and **5**). After 12 hours (0.5 days), weak AF488-CTB labeling was observed in the cell bodies of both types of neuron, as well as in the primary dendritic arbors of the motor neurons (**Figures 4** and **5**). The intensity of the labeling was seen to increase on days 1 and 2 (**Figures 4** and **5**). On day 3, the spinal motor neurons' secondary and tertiary dendritic arbors could be clearly seen, similar to the images typically obtained following Golgi staining (**Figure 4**). This detailed morphology was also apparent on days 5 and 7 (**Figure 4**). On day 14, however, most of the fluorescent neuronal labeling had faded to give a punctate appearance, especially on the dendritic arbors (**Figures 4** and **5**).

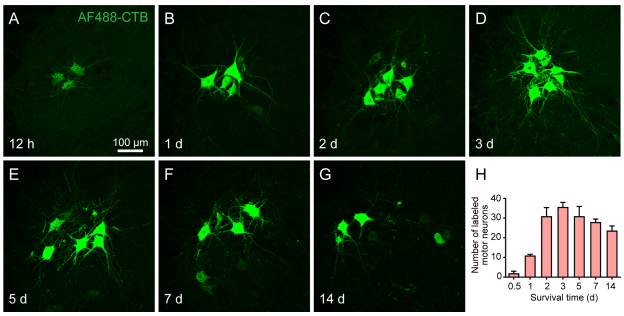

Figure 4 | Distribution and morphological characteristics of the labeled motor neurons at sequential time points following the injection of AF488-CTB into the gastrocnemius muscle.
(A–G) Representative sections from the spinal cord at the lumbar 4 segment showing the morphology of labeled motor neurons at (A) 12 hours, (B) 1 day, (C) 2 days, (D) 3 days, (E) 5 days, (F) 7 days, and (G) 14 days post-injection. Weak AF488-CTB labeling could be seen in the motor neuron cell bodies and primary dendritic arbors at 12 hours (A); the intensity increased on days 1 and 2 (B, C); on day 3, the secondary and tertiary dendritic arbors could be clearly seen (D); this detail was maintained on days 5 and 7 (E, F); on day 14, most of the fluorescent labeling had faded, giving a punctate appearance, especially on the dendritic arbors (G). The images were obtained from an experiment that used three rats per time point. Scale bar: 100 μm. (H) Average number of labeled motor neurons at different time points post-injection. The motor neurons were counted in every sixth slice of spinal cord. Data are expressed as the mean ± SEM (n = 3). AF: Alexa Fluor; CTB: cholera toxin subunit B.

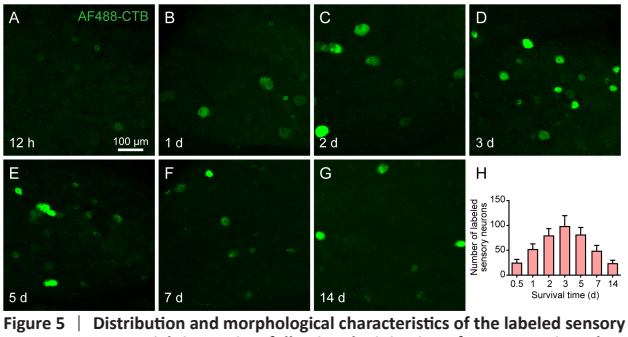

Figure 5 | Distribution and morphological characteristics of the labeled sensory neurons at sequential time points following the injection of AF488-CTB into the gastrocnemius muscle.
(A–G) Representative sections from the dorsal root ganglion at the lumbar 5 segment showing the morphology of labeled sensory neurons at (A) 12 hours, (B) 1 day, (C) 2 days, (D) 3 days, (E) 5 days, (F) 7 days, and (G) 14 days post- injection. Weak AF488-CTB labeling could be observed in the sensory neuron cell bodies at 12 hours (A); the intensity increased on days 1 and 2 (B, C); on day 3, the sensory neurons could be clearly seen (D); this detail was maintained on days 5 and 7 (E, F); on day 14, most of the fluorescent labeling had faded, giving a punctate appearance (G). The images were obtained from an experiment that used three rats per time point. Scale bar: 100 μm. (H) Average number of labeled sensory neurons at different time points post-injection. The sensory neurons were counted in the whole-mount DRG. Data are expressed as the mean ± SEM (n = 3). AF: Alexa Fluor; CTB: cholera toxin subunit B.

Neurochemical substances in the labeled neurons

Certain neurochemical substances were examined in the labeled neurons and compared between days 3 and 14 following the AF488-CTB injection. It was found that there were no marked changes in CGRP expression in the labeled motor and sensory neurons (**Figure 6**), nor in ChAT expression in the labeled motor neurons (**Figure 7**), even though the AF488-CTB labeling faded with time. Nissl-labeling of the AF488-CTB neurons was also found to be similar to that seen in the unlabeled neurons (**Figures 6** and **7**).

Potential pathological changes around the labeled neurons

We found that Cl Casp-3 was distributed around the AF488-CTB-labeled neurons forming a dotted pattern (**Figure 8**). There were no obvious differences between days 3 and 14. The microglia were labeled with CD11b and were shown to have small cell bodies and thin cellular processes. They were evenly distributed around the labeled motor neurons, and there were no marked morphological differences between days 3 and 14; it was also found that they were similar to the microglia around the unlabeled motor neurons in the corresponding contralateral area (**Figure 8**).

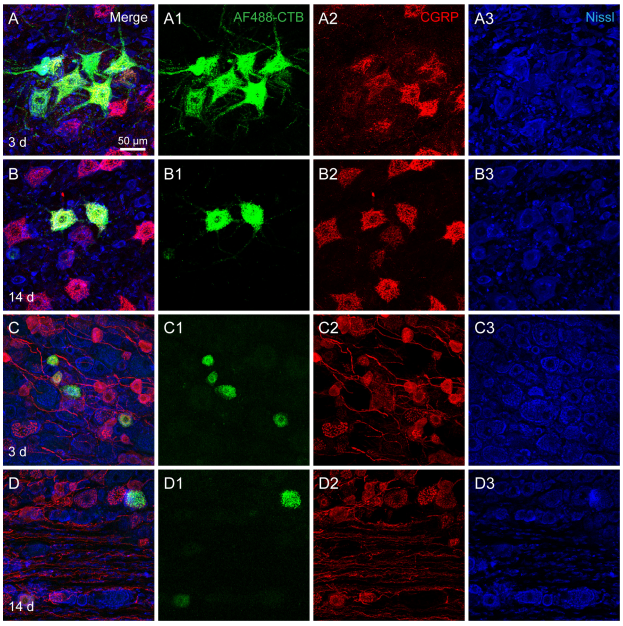

Figure 6 | CGRP expression in AF488-CTB-labeled motor and sensory neurons on days 3 and 14 post-injection.
(A–D) Representative sections from (A, B) the spinal cord at the lumbar 4 segment and (C, D) the dorsal root ganglion at the lumbar 5 segment (C, D). The sections show CGRP expression in the labeled motor (A, B) and sensory neurons (C, D) on day 3 (A, C) and day 14 (B, D) post-injection. The AF488-CTB labeling was seen to fade on day 14 (B, D), but there were no marked changes in the expression of CGRP in either the motor or the sensory neurons (A–D). (A1–D1, A2–D2, and A3–D3) The panels A–D are shown separately for AF488-CTB (A1–D1), CGRP (A2–D2), and Nissl (A3–D3). The images were obtained from an experiment that used three rats per time point. Scale bar: 50 μm. AF: Alexa Fluor; CGRP: calcitonin gene-related peptide; CTB: cholera toxin subunit B.

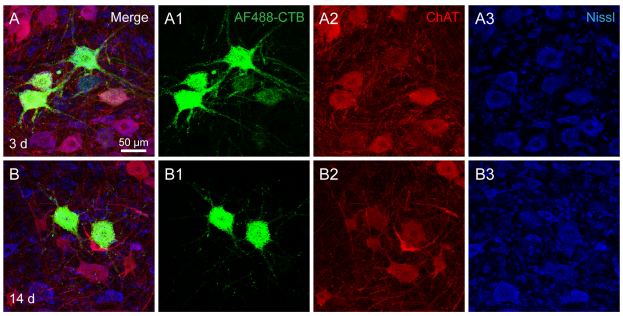

Figure 7 | ChAT expression in AF488-CTB-labeled motor neurons on days 3 and 14 post-injection.
(A–B) Representative sections of the spinal cord at the lumbar 4 segment, which show ChAT expression in the AF488-CTB-labeled motor neurons on (A) day 3 and (B) day 14 post-injection. The AF488-CTB labeling faded on day 14 (B), but there were no marked changes in the expression of ChAT (A, B). (A1–B1, A2–B2, and A3–B3) The panels A and B are shown separately for AF488-CTB (A1–B1), ChAT (A2–B2), and Nissl (A3–B3). The images were obtained from an experiment that used three rats per time point. Scale bar: 50 μm. AF: Alexa Fluor; ChAT: choline acetyltransferase; CTB: cholera toxin subunit B.

Discussion

In this study, we examined the use of AF488-CTB for the retrograde tracing of motor, sensory, and sympathetic neurons associated with the gastrocnemius muscle in the rat. As a sensitive retrograde tracer, AF488-CTB can be used for tracing the innervation patterns of a particular muscle, or, when used together with AF594-CTB, for comparing the innervation patterns of different muscles. Our study showed that there is an optimal time-window for visualizing AF488-CTB-labeled neurons in morphological detail. In addition, we found that certain neurochemical substances were unaffected by the labeling and that there were no signs of pathology.

Technological considerations

CTB has previously been used as a neural tracer, both in its unconjugated form and when conjugated with horseradish peroxidase, for the anterograde, retrograde, and transganglionic tracing of neural pathways (Hirakawa et al., 1992; Ciriello and Caverson, 2016; Dong et al., 2017; Wang et al., 2018; Cui et al., 2019; Han et al., 2019; Ma et al., 2020). The AF-CTB conjugates were developed more recently and have the advantage of being robust and photostable (Conte et al., 2009); they have now been used extensively in retrograde tracing studies (Conte et al., 2009; Cui et al., 2013; Zhang et al., 2021). AF-CTB labeling can be directly visualized in tissue sections, and even in transparent, whole-mount DRG and sympathetic chains. This stands in contrast to unconjugated CTB, which needs to be stained using complex

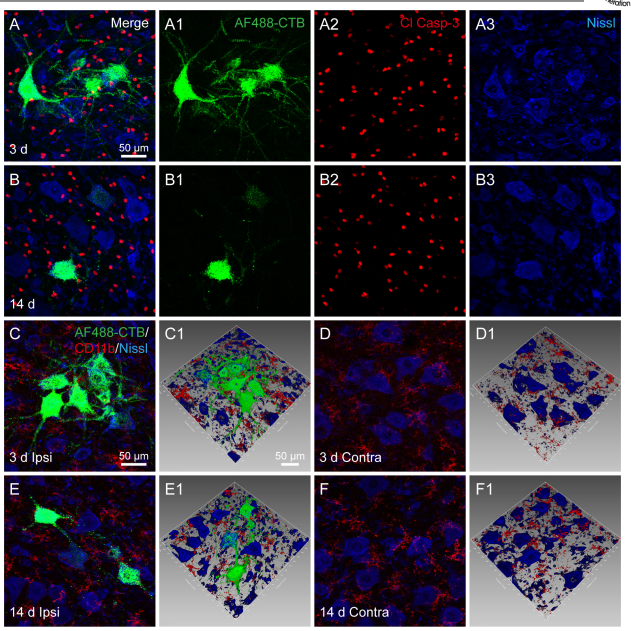

Figure 8 | Cl Casp-3 expression and microglia around the AF488-CTB-labeled motor neurons and unlabeled comparison neurons on days 3 and 14 post-injection.
(A, B) Representative sections of the spinal cord at the lumbar 4 segment showing Cl Casp-3 expression around the labeled motor neurons on (A) day 3 and (B) day 14 post-injection. (A1–3 and B1–3) The panels A and B are shown separately for AF488-CTB (A1, B1), Cl Casp-3 (A2, B2), and Nissl (A3, B3). The images did not reveal any obvious differences in Cl Casp-3 expression between days 3 and 14. (C–F) Representative sections of the spinal cord at the lumbar 4 segment showing CD11b-positive microglia around (C, E) the AF488-CTB-labeled motor neurons and (D, F) the contralateral unlabeled motor neurons on day 3 (C, D) and day 14 (E, F). (C1–F1) Adjusted images from panels C–F with three-dimensional reconstruction in a sloping pattern. These show the spatial detail between the microglia and the motor neurons. The microglia were seen to be evenly distributed around the labeled motor neurons, and there were no marked morphological differences between days 3 and 14 (C, E); the results were similar for the microglia around the unlabeled motor neurons on the contralateral side (D, F). The images were obtained from two independent experiments that used three rats per time point. Scale bars: 50 μm. AF: Alexa Fluor; Contra: contralateral; Cl Casp-3: cleaved caspase-3; CTB: cholera toxin subunit B; Ipsi: ipsilateral.

immunoperoxidase or immunofluorescence techniques (Hirakawa et al., 1992; Wang et al., 2018; Cui et al., 2019). This therefore enables researchers to rapidly assess whether tracing has been successful or not, and to avoid time-consuming tissue slicing.

In our study, we were able to visualize the neuromuscular junctions in the gastrocnemius muscle around the injection site. The axon terminals and motor endplates were labeled with AF488-CTB and α-bungarotoxin, respectively, and revealed the typical structure of neuromuscular junctions (Chen et al., 2016; Yin et al., 2019). This finding indicates that AF488-CTB is directly taken up by the axon terminals and then transported retrogradely to the neurons.

We examined the labeling efficiency of AF488-CTB when used alone or alongside AF594-CTB. We found that the motor, sensory, and sympathetic neurons associated with the gastrocnemius muscle were only distributed within their corresponding regions and segments, and were distinct from those associated with the tibialis anterior muscle. This was observed in the spinal cord, DRG, and sympathetic chain, and the pattern implies that AF488-CTB and AF594-CTB have similar properties for tracing from the peripheral nervous system to the central nervous system. Compared with other types of fluorescent tracers (Byers et al., 2002; Katada et al., 2006; Yu et al., 2015), these markers would appear to be particularly suitable for dual-tracing experiments involving the peripheral nervous system (Cui et al., 2013; Zhang et al., 2021).

It should be noted that, unlike unconjugated CTB and CTB conjugated with horseradish peroxidase (Hirakawa et al., 1992; Panneton et al., 2005; Cui et al., 2019), AF-CTB cannot be transported through the sensory pathway across the ganglia to label the terminals in the gracile nucleus, Clarke's nucleus, and spinal dorsal horn in adult rats (**Additional Figure 1**; Cui et al., 2013; Zhang et al., 2021). Nevertheless, a recent study showed that AF-CTB can be effectively used to label the terminals of sensory neurons in young mice (Li et al., 2011), which involves transportation across the sensory ganglia, thus implying that the labeling may depend upon the animal's age and species.

Changes in neuronal labeling over time

The labeling efficiency of neuronal tracers is affected by many factors, including the dose, concentration, injection procedure, post-injection time, and distance between the injection site and the target area (Vercelli et al., 2000; Lanciego and Wouterlood, 2011, 2020; Ling et al., 2012). We found that AF488-CTB labeling can be observed as early as 12 hours post-injection and for as long as 14 days; however, the optimal time-window was from day

3 to day 7 post-injection, when the images were of a higher quality. Previous studies have identified similar optimal time windows for unconjugated CTB (Hirakawa et al., 1992) and for other types of tracers (Han et al., 2012; Ling et al., 2012; Zhang et al., 2017). For the early time points post-injection, it is plausible that the neurons may not have taken up enough of the tracer; for the later time points, the neuronal labeling may have faded due to cellular metabolism (Puigdellívol-Sánchez et al., 2002; Yu et al., 2015; Zhang et al., 2017). Taken together, these results show that it is important to be aware of the labeling changes over time to obtain high quality images for neuronal tracing.

We were able to demonstrate changes in AF488-CTB labeling using a series of time points post-injection. We reasoned that the neuronal connections between the tracer injection site and the target regions should not be affected by any morphological changes in the labeled neurons over time; however, by studying the neuronal structure in more detail, it may be possible to observe signs of pathology in the labeled neurons (Lanciego and Wouterlood, 2011, 2020).

Neurochemical substances and microglial activation

We investigated whether there were any signs of pathology in the AF488-CTB-labeled neurons. For this, we selected CGRP, ChAT, Cl Casp-3, and CD11b to evaluate certain neurochemical substances and the microglial morphology around the labeled neurons. These were assessed at both early and later time points post-injection.

As a neuropeptide, CGRP is involved in neuromodulation and neurotrophy. There is evidence that it may also be involved in motor and sensory neuron pathology (Zheng et al., 2008; Chen et al., 2010; Li et al., 2019). In this study, we found that there were no marked differences in CGRP expression between the AF488-CTB-labeled neurons and unlabeled neurons; there were also no differences between the early and later stages post-injection. This finding implies that the labeled neurons were functioning normally. We also examined ChAT in the spinal cord. This enzyme catalyzes acetylcholine synthesis, and it is found in motor neurons along with CGRP (Das et al., 2021). We found that ChAT was expressed similarly in the labeled and unlabeled neurons, and also at the different time points. This therefore also implies that the AF488-CTB-labeled motor neurons were functioning normally.

In addition to the neurochemical substances, we also examined other potential signs of pathology in the labeled neurons and their surrounding glial cells using Cl Casp-3 and CD11b (Köbbert and Thanos, 2000; Beggs and Salter, 2007; Aras et al., 2012; Hickman et al., 2018; Li et al., 2019). We found that there were no marked differences in Cl Casp-3 and CD11b expression between the early and later time points. This implies that AF-CTB does not damage the labeled neurons. Because some fluorescent tracers can lead to functional impairments in the labeled neurons (Hu et al., 2013; Mi et al., 2019), this finding should encourage the more widespread use of AF-CTB for neural tract tracing. However, although we did not observe any signs of pathology in our AF-CTB labeled neurons, further histochemical studies should be carried out to examine this in more detail and confirm these findings.

Long-term fluorescence imaging *in vivo* is currently becoming more widespread (Chen et al., 2019). This was not carried out in the present study because of technical limitations, but this could be examined in future studies. However, this could prove challenging because the labeled motor neurons are located deep in the spinal ventral horn.

Conclusion

Our results provide evidence that both AF488-CTB and AF594-CTB are highly effective for retrograde tracing from muscular tissue. For optimal results, the labeling should be observed during a particular time window following the injection, so that the morphological detail of the labeled neurons can be clearly seen. This technique could be used to provide neuroanatomical information concerning neuronal connections, as well as to evaluate neuronal degeneration or regeneration following peripheral nerve damage.

Author contributions: *Study conception and design: JJC, WZB; neural tracer injection: JJC, JW, DSX, YTG, YHL; histochemical staining and sample observation: JJC, JW, SW, YXS, YQW; data analysis and figure preparation: JW, DSX, XHJ; manuscript drafting: JJC, WZB. All authors approved the final manuscript.*
Conflicts of interest: *The authors declare no conflicts of interest.*
Availability of data and materials: *The data supporting the conclusions of this article will be made available from the corresponding author on reasonable request.*

Open peer reviewers: *José L. Lanciego, University of Navarra, Spain; Arjun Singh, Memorial Sloan-Kettering Cancer Center, USA.*
Additional files:
Additional file 1: *Open peer review report 1.*
Additional Figure 1: *Distribution of labeled motor neurons, sensory neurons and transganglionic axonal terminals on the third day after injection of CTB into the gastrocnemius muscle.*

References

Aras R, Barron AM, Pike CJ (2012) Caspase activation contributes to astrogliosis. Brain Res 1450:102-115.
Beggs S, Salter MW (2007) Stereological and somatotopic analysis of the spinal microglial response to peripheral nerve injury. Brain Behav Immun 21:624-633.
Byers CT, Fan R, Messina A, Morrison WA, Galea MP (2002) Comparing the efficacy of two fluorescent retrograde tracers in labeling the motor and sensory neuron populations of the rat sciatic nerve. J Neurosci Methods 114:159-164.
Chen C, Zhang J, Sun L, Zhang Y, Gan WB, Tang P, Yang G (2019) Long-term imaging of dorsal root ganglia in awake behaving mice. Nat Commun 10:3087.
Chen LJ, Zhang FG, Li J, Song HX, Zhou LB, Yao BC, Li F, Li WC (2010) Expression of calcitonin gene-related peptide in anterior and posterior horns of the spinal cord after brachial plexus injury. J Clin Neurosci 17:87-91.
Chen W, Yu T, Chen B, Qi Y, Zhang P, Zhu D, Yin X, Jiang B (2016) In vivo injection of α-bungarotoxin to improve the efficiency of motor endplate labeling. Brain Behav 6:e00468.
Ciriello J, Caverson MM (2016) Effect of estrogen on vagal afferent projections to the brainstem in the female. Brain Res 1636:21-42.
Conte WL, Kamishina H, Reep RL (2009) Multiple neuroanatomical tract-tracing using fluorescent Alexa Fluor conjugates of cholera toxin subunit B in rats. Nat Protoc 4:1157-1166.
Cui J, Wang J, Bai W (2019) Innervated properties of acupuncture points LI 4 and LR 3 in the rat: neural pathway tracing with cholera toxin subunit B. Med Acupunct 31:169-175.
Cui J, Ha L, Zhu X, Wang F, Jing X, Bai W (2013) Specificity of sensory and motor neurons associated with BL40 and GB30 in the rat: a dual fluorescent labeling study. Evid Based Complement Alternat Med 2013:643403.
Das S, Nalini A, Laxmi TR, Raju TR (2021) ALS-CSF-induced structural changes in spinal motor neurons of rat pups cause deficits in motor behaviour. Exp Brain Res 239:315-327.
Dong X, Li S, Kirouac GJ (2017) Collateralization of projections from the paraventricular nucleus of the thalamus to the nucleus accumbens, bed nucleus of the stria terminalis, and central nucleus of the amygdala. Brain Struct Funct 222:3927-3943.
Han S, Li D, Kou Y, Fu Z, Yin X (2019) Multiple retrograde tracing methods compatible with 3DISCO clearing. Artif Cells Nanomed Biotechnol 47:4240-4247.
Han X, Lv G, Wu H, Ji D, Sun Z, Li Y, Tang L (2012) Biotinylated dextran amine anterograde tracing of the canine corticospinal tract. Neural Regen Res 7:805-809.
Hickman S, Izzy S, Sen P, Morsett L, El Khoury J (2018) Microglia in neurodegeneration. Nat Neurosci 21:1359-1369.
Hirakawa M, McCabe JT, Kawata M (1992) Time-related changes in the labeling pattern of motor and sensory neurons innervating the gastrocnemius muscle, as revealed by the retrograde transport of the cholera toxin B subunit. Cell Tissue Res 267:419-427.
Hu W, Liu D, Zhang Y, Shen Z, Gu T, Gu X, Gu J (2013) Neurological function following intra-neural injection of fluorescent neuronal tracers in rats. Neural Regen Res 8:1253-1261.
Juavinett AL, Kim EJ, Collins HC, Callaway EM (2020) A systematic topographical relationship between mouse lateral posterior thalamic neurons and their visual cortical projection targets. J Comp Neurol 528:95-107.
Katada A, Vos JD, Swelstad BB, Zealear DL (2006) A sequential double labeling technique for studying changes in motoneuronal projections to muscle following nerve injury and reinnervation. J Neurosci Methods 155:20-27.
Köbbert C, Thanos S (2000) Topographic representation of the sciatic nerve motor neurons in the spinal cord of the adult rat correlates to region-specific activation patterns of microglia. J Neurocytol 29:271-283.
Lanciego JL, Wouterlood FG (2011) A half century of experimental neuroanatomical tracing. J Chem Neuroanat 42:157-183.
Lanciego JL, Wouterlood FG (2020) Neuroanatomical tract-tracing techniques that did go viral. Brain Struct Funct 225:1193-1224.
Li L, Rutlin M, Abraira VE, Cassidy C, Kus L, Gong S, Jankowski MP, Luo W, Heintz N, Koerber HR, Woodbury CJ, Ginty DD (2011) The functional organization of cutaneous low-threshold mechanosensory neurons. Cell 147:1615-1627.
Li YZ, Miao RP, Yu TY, Bai WZ, Cui JJ, Lu MQ, Shen Y, Luo YT, Shao S, Zhang YM, Mo YJ, Lv TT, Chen GY (2019) Mild mechanic stimulate on acupoints regulation of CGRP-positive cells and microglia morphology in spinal cord of sciatic nerve injured rats. Front Integr Neurosci 13:58.
Lin SD, Tang T, Zhao TB, Liu SJ (2017) Central projections and connections of lumbar primary afferent fibers in adult rats: effectively revealed using Texas red-dextran amine tracing. Neural Regen Res 12:1695-1702.
Ling C, Hendrickson ML, Kalil RE (2012) Resolving the detailed structure of cortical and thalamic neurons in the adult rat brain with refined biotinylated dextran amine labeling. PLoS One 7:e45886.
Ma L, Chen W, Yu D, Han Y (2020) Brain-wide mapping of afferent inputs to accumbens nucleus core subdomains and accumbens nucleus subnuclei. Front Syst Neurosci 14:15.
Mi D, Yuan Y, Zhang Y, Niu J, Wang Y, Yan J, Yang Y, Hu W (2019) Injection of Fluoro-Gold into the tibial nerve leads to prolonged but reversible functional deficits in rats. Sci Rep 9:9906.
Panneton WM, Gan Q, Juric R (2005) The central termination of sensory fibers from nerves to the gastrocnemius muscle of the rat. Neuroscience 134:175-187.
Percie du Sert N, Hurst V, Ahluwalia A, Alam S, Avey MT, Baker M, Browne WJ, Clark A, Cuthill IC, Dirnagl U, Emerson M, Garner P, Holgate ST, Howells DW, Karp NA, Lazic SE, Lidster K, MacCallum CJ, Macleod M, Pearl EJ, et al. (2020) The ARRIVE guidelines 2.0: Updated guidelines for reporting animal research. PLoS Biol 18:e3000410.
Puigdellívol-Sánchez A, Valero-Cabré A, Prats-Galino A, Navarro X, Molander C (2002) On the use of fast blue, fluoro-gold and diamidino yellow for retrograde tracing after peripheral nerve injury: uptake, fading, dye interactions, and toxicity. J Neurosci Methods 115:115-127.
Sargsyan SA, Monk PN, Shaw PJ (2005) Microglia as potential contributors to motor neuron injury in amyotrophic lateral sclerosis. Glia 51:241-253.
Sarkar DK, Mitsugi N (1990) Correlative changes of the gonadotropin-releasing hormone and gonadotropin-releasing-hormone-associated peptide immunoreactivities in the pituitary portal plasma in female rats. Neuroendocrinology 52:15-21.
Stevenson ME, Lensmire NA, Swain RA (2018) Astrocytes and radial glia-like cells, but not neurons, display a nonapoptotic increase in caspase-3 expression following exercise. Brain Behav 8:e01110.
Vercelli A, Repici M, Garbossa D, Grimaldi A (2000) Recent techniques for tracing pathways in the central nervous system of developing and adult mammals. Brain Res Bull 51:11-28.
Wang J, Cui J, She C, Xu D, Zhang Z, Wang H, Bai W (2018) Differential innervation of tissues located at traditional acupuncture points in the rat forehead and face. Acupunct Med 36:408-414.
Xu J, Xuan A, Liu Z, Li Y, Zhu J, Yao Y, Yu T, Zhu D (2021) An approach to maximize retrograde transport based on the spatial distribution of motor endplates in mouse hindlimb muscles. Front Cell Neurosci 15:707982.
Yin X, Yu T, Chen B, Xu J, Chen W, Qi Y, Zhang P, Li Y, Kou Y, Ma Y, Han N, Wan P, Luo Q, Zhu D, Jiang B (2019) Spatial distribution of motor endplates and its adaptive change in skeletal muscle. Theranostics 9:734-746.
Yu YL, Li HY, Zhang PX, Yin XF, Han N, Kou YH, Jiang BG (2015) Comparison of commonly used retrograde tracers in rat spinal motor neurons. Neural Regen Res 10:1700-1705.
Zhang W, Xu D, Cui J, Jing X, Xu N, Liu J, Bai W (2017) Anterograde and retrograde tracing with high molecular weight biotinylated dextran amine through thalamocortical and corticothalamic pathways. Microsc Res Tech 80:260-266.
Zhang Z, Xu D, Wang J, Cui J, Wu S, Zou L, Shen Y, Jing X, Bai W (2021) Correlated sensory and sympathetic innervation between the acupoint BL23 and kidney in the rat. Front Integr Neurosci 14:616778.
Zheng LF, Wang R, Xu YZ, Yi XN, Zhang JW, Zeng ZC (2008) Calcitonin gene-related peptide dynamics in rat dorsal root ganglia and spinal cord following different sciatic nerve injuries. Brain Res 1187:20-32.

P-Reviewers: Lanciego JL, Singh A; C-Editor: Zhao M; S-Editors: Yu J, Li CH; L-Editors: Foxton J, Yu J, Song LP; T-Editor: Jia Y

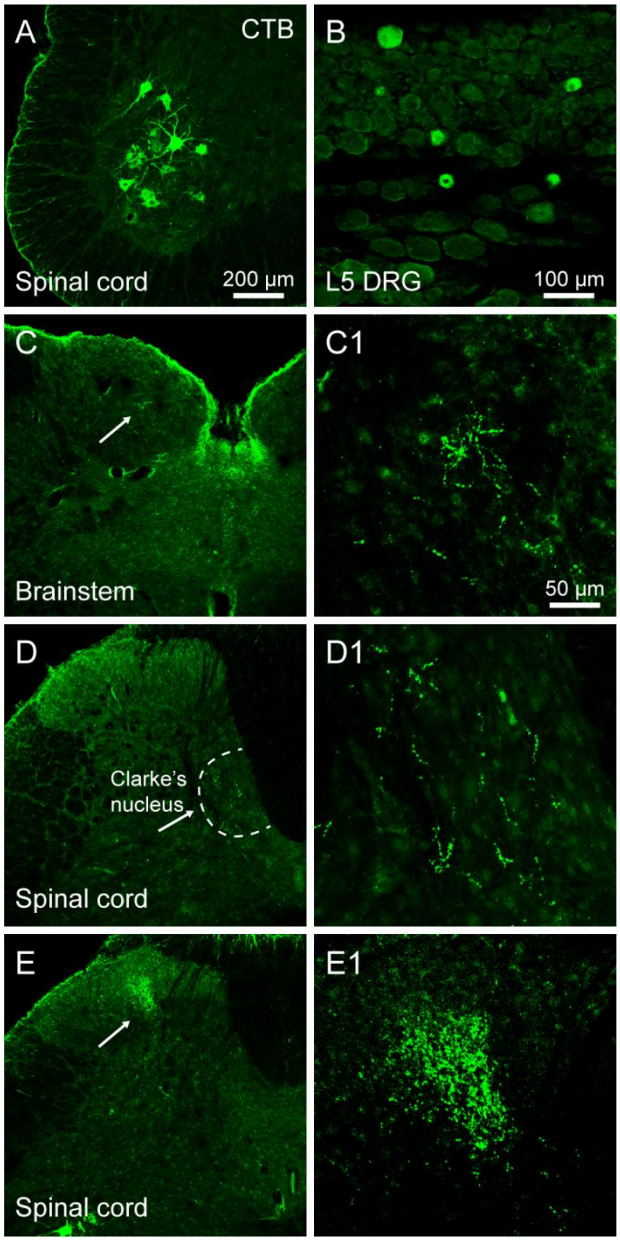

Additional Figure 1 Distribution of labeled motor neurons, sensory neurons and transganglionic axonal terminals on the third day after injection of CTB into the gastrocnemius muscle.

(A, B) CTB labeled motor neurons at lumbar (L) 4 segment spinal ventral horn (A) and sensory neurons in L5 segment dorsal root ganglion (DRG, B). (C-E) CTB labeled transganglionic axonal terminals in gracile nucleus (C), Clarke's nucleus (D) and the laminae III and V spinal dorsal horn (E). (C1-E1) Higher magnified photo from panels C-E (arrow heads) showing the labeled transganglionic axonal terminals in detail respectively. One independent experiment was performed using three rats. Scale bars: 200 μm in A, C, D and E; 100 μm in B; 50 μm in C1, D1 and E1. AF: Alexa Fluor; CTB: cholera toxin subunit B.